AGN Physics with the Sloan Digital Sky Survey
*ASP Conference Series, Vol. **VOLUME***, 2004*
G.T. Richards and P.B. Hall

X-raying Active Galaxies Found and Missed by the Sloan Digital Sky Survey

W.N. Brandt, D.P. Schneider

Department of Astronomy & Astrophysics, The Pennsylvania State University, 525 Davey Lab, University Park, PA 16802, USA

C. Vignali

INAF-Osservatorio Astronomico di Bologna, Via Ranzani, 1, 40127 Bologna, Italy

Abstract. Current X-ray observatories, archival X-ray data, and the Sloan Digital Sky Survey (SDSS) represent a powerful combination for addressing key questions about active galactic nuclei (AGN). We describe a few selected issues at the forefront of X-ray AGN research and the relevance of the SDSS to them. Bulk X-ray/SDSS AGN investigations, X-ray weak AGN, red AGN, hard X-ray selected AGN, high-redshift AGN demography, and future prospects are all briefly discussed.

1. Introduction

X-ray emission appears to be a universal property of AGN, and many AGN emit a significant fraction of their total power in the X-ray band. As a result, X-ray surveys have proved powerful in finding AGN; they minimize absorption biases and dilution by host-galaxy light. X-ray surveys have found the highest known sky densities of AGN; in the *Chandra* Deep Field-North (CDF-N) and South (CDF-S) the AGN density is $\gtrsim 5000$ deg^{-2}, about an order of magnitude higher than for the deepest small-area AGN surveys in the optical.

Detailed X-ray spectral and variability studies probe the immediate vicinity of the central black hole, where accretion and black hole growth occur, as well as the larger scale nuclear environment. Primary X-ray continuum components include a hard power law, a soft X-ray excess, and a "reflection" continuum; these are thought to be collectively generated by the inner accretion disk (within $\approx$ 10–100 Schwarzschild radii) and a hot disk corona, and they can show rapid and large-amplitude variability on timescales down to $\approx$ 100–1000 s. Radio-loud AGN additionally show power-law emission associated with jet-linked X-rays. Many atomic spectral features are also observed including lines and edges from ionized outflows and a fluorescent iron Kα line associated with the "reflection" process (see Fig. 1 for an example).

Current X-ray observatories (e.g., *Chandra* and *XMM-Newton*), archival X-ray data (e.g., the thousands of observations made by *ASCA*, *BeppoSAX*, and *ROSAT*), and the SDSS represent a powerful combination for addressing key questions about AGN. The SDSS has already demonstrated its power as

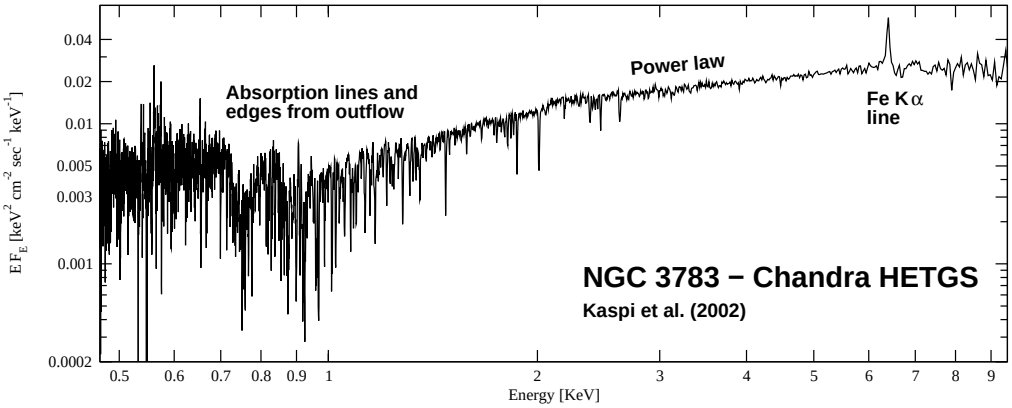

Figure 1. *Chandra* High-Energy Transmission Grating Spectrometer 900 ks spectrum of the Seyfert 1 galaxy NGC 3783 illustrating absorption lines and edges associated with an ionized outflow ($\approx$ 140 such features are detected), the underlying power-law continuum, and the Fe Kα line. The resolving power is $E/\Delta E \approx$ 250–1500 over most of the plotted spectral range. Adapted from Kaspi et al. (2002).

an X-ray source identification "machine" and has also generated large and well-defined AGN samples for X-ray follow-up studies. Below we will describe a few selected issues at the forefront of X-ray AGN research and the relevance of the SDSS to them. Only limited citations will be possible due to finite space; our apologies in advance.

2. Bulk Follow-Up Work and AGN X-ray Evolution

2.1. Bulk SDSS Identification of X-ray Sources

The SDSS spectroscopic survey is well matched in depth and sky density to the *ROSAT* All-Sky Survey (RASS). Anderson et al. (2003) describe plans to identify $\approx 10,000$ of the $\approx 100,000$ RASS sources using the SDSS; objects in RASS error circles with unusual SDSS colors or FIRST radio detections are targeted. Thus far an impressive $\approx$ 1200 AGN (about 80% new) found in 1400 deg^2 have been delivered ($\approx$ 964 broad-line AGN, $\approx$ 216 intermediate AGN and Seyfert 2 candidates, and $\approx$ 45 likely BL Lacs). The ultimate order-of-magnitude increase in sample size compared to the largest previous X-ray source identification programs will allow (1) studies of AGN X-ray evolution in the smallest possible luminosity and redshift bins, and (2) significantly improved statistical studies of minority X-ray AGN populations. Many bright ($g < 17$) AGN are being discovered that deserve targeted follow-up studies.

2.2. Bulk X-ray Investigation of SDSS Sources

Vignali, Brandt, & Schneider (2003a) have pursued a complementary program: X-ray investigation of SDSS AGN serendipitously lying in pointed *ROSAT* fields. In this case, the focus is on optically selected (rather than X-ray selected) AGN.

This approach generates X-ray/SDSS matches not found by Anderson et al. (2003) because (1) the SDSS AGN density on the sky is several times higher than the RASS X-ray source density, and (2) pointed *ROSAT* observations are typically 2–10 times more sensitive than the RASS. Vignali et al. (2003a) find that $\approx 3.2\%$ of the 462 deg^2 SDSS Early Data Release (EDR) area has sensitive coverage in pointed *ROSAT* observations; this study presents pointed *ROSAT* results for 128 of the EDR AGN in the Schneider et al. (2002) catalog. This basic approach has large growth potential; ultimately ≈ 2700 SDSS AGN are expected to have serendipitous pointed *ROSAT* coverage.

2.3. AGN X-ray Evolution

The bulk follow-up work summarized above enables multiple science projects, including investigations of the cosmic evolution of AGN X-ray emission. Such investigations can ultimately determine if AGN black holes feed and grow in the same way at all cosmic epochs, and they have a long history going back to the 1980's (see Vignali et al. 2003a for a review). Generally, little X-ray evolution is found with redshift after luminosity effects are taken into account, although there have been some notable counterclaims.

Vignali et al. (2003a) have recently used their SDSS AGN sample to investigate the X-ray evolution of radio-quiet AGN. Their sample has several notable advantages compared to previous work: (1) it has been optically selected in a well-defined manner and spans large ranges of redshift ($z = 0.16$–6.28) and luminosity, (2) it has sensitive radio coverage from FIRST and NVSS enabling effective selection of only radio-quiet AGN, and (3) it allows the effects of Broad Absorption Line (BAL) quasars, which often suffer from strong X-ray absorption, to be minimized and controlled. Partial correlation analyses using the parameter $\alpha_{\rm ox}$ (the slope of a nominal power law between rest-frame 2500 Å and 2 keV) indicate no significant dependence of $\alpha_{\rm ox}$ upon redshift after controlling for an observed dependence of $\alpha_{\rm ox}$ upon 2500 Å luminosity density (l_{2500}). This strengthens and broadens earlier similar conclusions, demonstrating that the small-scale X-ray emission regions of most luminous AGN are remarkably stable from $z \approx 0$–6 despite the strong large-scale environmental changes over this interval.

Anderson et al. (2003) have investigated the dependence of $\alpha_{\rm ox}$ upon l_{2500} using their X-ray selected sample of SDSS AGN. They suggest that the $\alpha_{\rm ox}$-log(l_{2500}) relation may be nonlinear, with (1) relatively little dependence of $\alpha_{\rm ox}$ upon l_{2500} for $l_{2500} \lesssim 10^{29.5}$ erg s^{-1} Hz^{-1}, and (2) a stronger dependence of $\alpha_{\rm ox}$ upon l_{2500} for $l_{2500} \gtrsim 10^{29.5}$ erg s^{-1} Hz^{-1}. Similar evidence for nonlinearity has been presented by Wilkes et al. (1994) and Yuan et al. (1998). This nonlinear dependence will need to be included in future studies of AGN X-ray evolution.

3. Selected Topics for Joint X-ray and SDSS Investigations

3.1. X-ray Weak AGN

Although X-ray emission appears to be a universal property of AGN, there are some notably X-ray weak AGN; these have $\alpha_{\rm ox} \gtrsim 1.75$–$2$ and lie on a "skew tail"

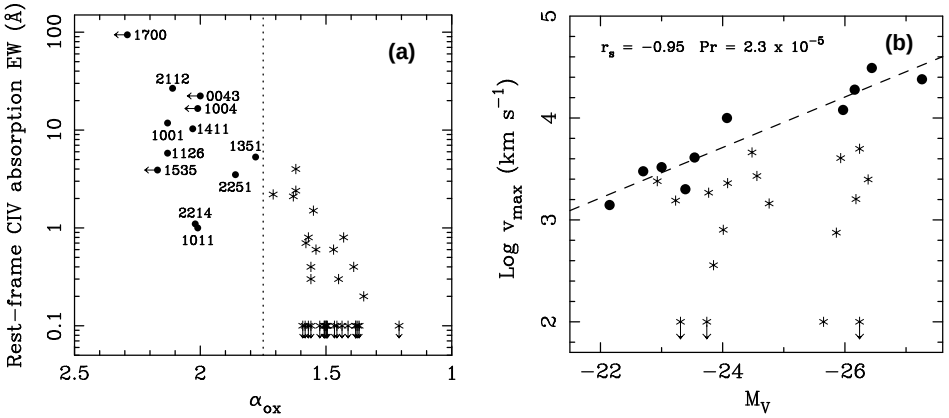

Figure 2. (a) C IV λ1549 absorption-line EW versus α_{ox} for the $z < 0.5$ BQS AGN. X-ray weak AGN (filled circles with $\alpha_{ox} > 1.75$) are designated by the right ascension parts of their names. Stars denote objects with weak or no X-ray and UV absorption. Adapted from BLW. (b) The luminosity (M_V) dependence of maximum UV absorption velocity (v_{max}) for $z < 0.5$ BQS AGN. X-ray weak AGN (filled circles with $\alpha_{ox} > 2$) have the largest v_{max} at any given luminosity. Stars denote BQS AGN with UV absorption that are not X-ray weak. The dashed line shows the best-fit relation between v_{max} and luminosity: $v_{max} \propto L^{0.62\pm0.08}$ (see §3.4 of Laor & Brandt 2002 for comparison with simple radiation-pressure driven outflow models). Adapted from Laor & Brandt (2002).

of the α_{ox} distribution.[1] X-ray weak AGN include even type 1 AGN where the view into the nucleus should not be blocked by the "torus" of AGN unification models. Such X-ray weakness could in principle be due to intrinsic X-ray absorption, a missing accretion-disk corona, or perhaps extreme X-ray variability. By determining the causes of X-ray weakness, we will refine our understanding of the universality of AGN X-ray emission.

Brandt, Laor, & Wills (2000; hereafter BLW) systematically investigated X-ray weak AGN in the $z < 0.5$ Bright Quasar Survey (BQS; Schmidt & Green 1983). X-ray weak AGN comprise $\approx$ 11–15% of this blue AGN sample depending upon the (somewhat arbitrary) α_{ox} cutoff. From an observed strong correlation between α_{ox} and the equivalent width (EW) of blueshifted C IV absorption (see Fig. 2a), BLW argued that X-ray absorption associated with an outflow is

[1]The appropriate α_{ox} cutoff to use when defining an X-ray weak AGN is somewhat arbitrary, and the cutoff is likely luminosity dependent (see §2.3). Aside from the "skew tail" toward large α_{ox}, the α_{ox} distribution for AGN of similar luminosity appears to be roughly Gaussian. A reasonable criterion for X-ray weakness is that α_{ox} should lie $> 2\sigma$ from the mean of this Gaussian. Alternatively, mixture-modeling or dip-test algorithms may be employed (see §2 of BLW).

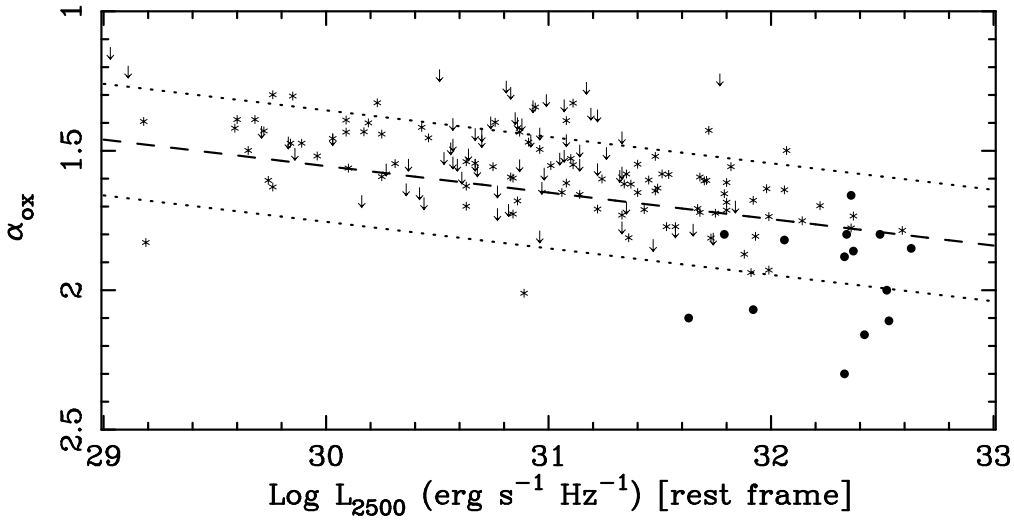

Figure 3. α_{ox} versus l_{2500} for SDSS radio-quiet AGN (stars and downward-pointing arrows denoting detections and upper limits, respectively; Vignali et al. 2003a) and the HQS AGN put forward by Risaliti et al. (2003) as X-ray weak (filled circles). The dashed line represents the best fit to the Vignali et al. (2003a, 2003b) data using censored analysis (see eqn. 4 of Vignali et al. 2003b), and the dotted lines show ± 0.2 intervals around the best fit.

likely the main cause of X-ray weakness for blue AGN.[2] This suspicion has been directly confirmed for several X-ray weak BQS AGN via X-ray spectroscopy (e.g., Brinkmann et al. 1999; Gallagher et al. 2001), although admittedly the spectroscopic sample size is limited.

It is also important to understand X-ray weakness in redder AGN; many of these were missed by the BQS. Risaliti et al. (2003) have recently investigated this issue using *Chandra* snapshot observations of 16 broad-line AGN from the grism-selected Hamburg Quasar Survey (HQS; e.g., Hagen et al. 1995). These AGN are somewhat redder than BQS AGN, and they generally do not show evidence for X-ray absorption. Risaliti et al. (2003) propose that these AGN are intrinsically underluminous in X-rays and thus have intrinsic spectral energy distributions (SEDs) different from those of "standard" blue AGN. The overall situation would then be perplexing with (1) X-ray weakness in blue AGN mainly being due to absorption, (2) X-ray weakness in somewhat redder AGN mainly being due to a different intrinsic SED, and (3) X-ray weakness in red AGN again mainly being due to absorption (see §3.2). One possible resolution lies in the issue of sample definition. Specifically, most of the Risaliti et al. (2003) AGN are highly luminous quasars, and many of these are only mildly X-ray weak compared to luminosity-dependent expectations for the range of α_{ox} (see Fig. 3). That is, many do not lie on the "skew tail" (see above) of the α_{ox}

[2]This correlation is also likely present for $z > 4$ quasars; see §4 of Vignali et al. (2003c) and references therein.

distribution but rather within the main body of this distribution. Thus, many of the Risaliti et al. (2003) AGN are not directly comparable to, for example, the BQS AGN studied by BLW.[3] The 4–5 Risaliti et al. (2003) AGN that do appear to be comparably X-ray weak have small numbers of counts (< 15 to 53) in their *Chandra* snapshot observations, and the current X-ray spectral data do not strongly constrain potentially complex X-ray absorption in these objects. Further studies of these objects are needed.

There are a few good candidates for intrinsically X-ray weak AGN. One notable example is PHL 1811, which shows no evidence for absorption even in high-quality *Chandra* and *HST* data (Leighly et al., these proceedings). Another, PG 1011–040, showed no evidence for X-ray absorption in an *ASCA* spectrum (Gallagher et al. 2001). The existence of these objects argues that X-ray absorption cannot universally explain X-ray weakness in AGN, and it is important to enlarge the sample of intrinsically X-ray weak AGN so that systematic studies are possible.

The SDSS AGN sample combined with sensitive archival X-ray data should be able to improve our understanding of X-ray weak AGN significantly. Ultimately a few hundred X-ray weak SDSS AGN should be identified spanning broad ranges of optical/near-infrared color, luminosity, and redshift, and follow-up studies of this large sample should definitively determine the causes of X-ray weakness. Furthermore, it should be possible to quantify the luminosity dependence of AGN outflows properly. Laor & Brandt (2002) found that X-ray weak BQS AGN have the highest maximum UV absorption velocity ($v_{\rm max}$) at any given luminosity ($M_{\rm V}$), and they suggested that $v_{\rm max}$ is largely set by luminosity as expected for radiation-pressure driven outflows (see Fig. 2b). Refinement of such relations using SDSS AGN has the potential to provide a unified understanding of AGN outflows ranging from Seyfert ionized absorbers to BAL quasars.

3.2. Red AGN

Moving to redder optical/near-infrared colors, significant X-ray attention has recently been lavished upon 2MASS AGN with $J - K_{\rm s} > 2$. These objects appear to have a space density comparable to previously known blue AGN; about 80% (20%) are type 1 (type 2). Snapshot *Chandra* observations of ≈ 46 of these objects reveal that they are generally X-ray weak (see Fig. 4a) and suggest that their hard X-ray spectra are probably caused by intrinsic X-ray absorption with $N_{\rm H} \approx 10^{21}$–$10^{23}$ cm^{-2} (Wilkes et al. 2002). There appears to be little relation between the estimated amount of X-ray absorption and near-infrared color, AGN classification, or optical polarization; hopefully X-ray and UV spectroscopy will clarify the nature of the absorption.

Additional selection methods can broaden our understanding of red AGN and allow X-ray studies out to high redshift; the Wilkes et al. (2002) sample has a small median redshift of $z \approx 0.2$. Richards et al. (2003) have presented a complementary approach advocating the use of relative (rather than observed) SDSS colors that remove redshift-dependent emission-line effects (see Fig. 4b). Their

[3]The application of a more stringent $\alpha_{\rm ox}$ criterion would also significantly reduce the remarkably high fraction ($\gtrsim 50\%$) of X-ray weak HQS AGN found by Risaliti et al. (2003).

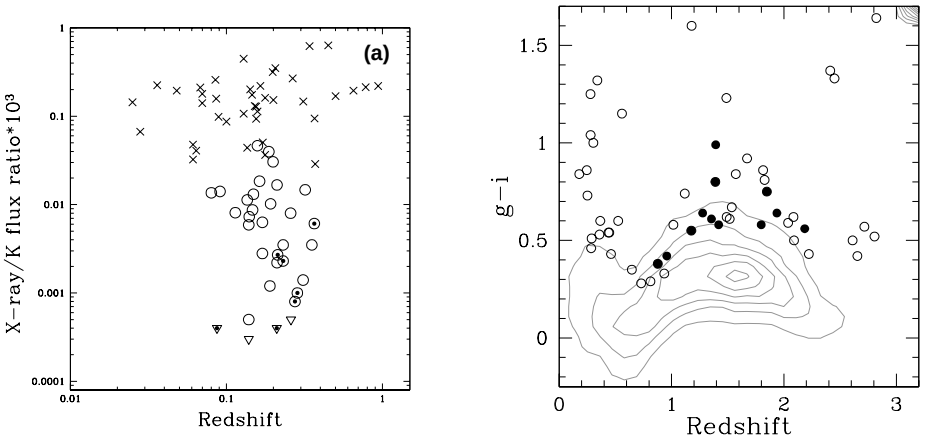

Figure 4. (a) Observed X-ray (1 keV) to K_s flux ratio versus redshift for 2MASS red AGN (circles) and low-redshift, broad-line AGN (crosses). Upper limits are indicated by triangles, and the reddest sources with $J - K_s > 2.5$ are indicated by an enclosed square. From B.J. Wilkes (2003, private communication); updated from Wilkes et al. (2002). (b) Observed $g - i$ color distribution of SDSS EDR AGN as a function of redshift (contours). The circles are SDSS red AGN; filled circles denote the 12 accepted for *Chandra* snapshot observations. Many of the reddest AGN are BAL quasars and thus were not selected as *Chandra* targets. From G.T. Richards (2003, private communication).

technique (1) allows detection of more subtle reddening than for the 2MASS red AGN, (2) provides a more meaningful quantification of the amount of reddening, and (3) allows high-redshift red AGN to be found effectively. *Chandra* snapshot observations have now been accepted for 12 of these SDSS red AGN at $z = 0.88$–2.19, and comparisons with the 2MASS red AGN should be enlightening.

3.3. Hard X-ray Selected AGN

Sensitive hard X-ray surveys reveal a wide variety of AGN. In addition to the standard type 1 and type 2 AGN, a class of X-ray bright, optically normal galaxies (XBONGs) is detected (e.g., Barger et al. 2001; Hornschemeier et al. 2001; Comastri et al. 2002a,b). XBONGs can have hard X-ray spectra and X-ray luminosities of $\approx 10^{41}$–10^{43} erg s^{-1}. Optical spectra give redshifts of $z \approx 0.05$–1, but AGN emission lines and non-stellar continua are not apparent. Some XBONGs may just be Seyfert 2s where dilution by host-galaxy light hinders optical detection of the AGN (e.g., Moran et al. 2002; Severgnini et al. 2003), but others have high-quality follow up and appear to be truly remarkable (e.g., Comastri et al. 2002a). The place of the "true" XBONGs in the AGN unified model remains unclear; they may suffer from heavy obscuration covering a large solid angle ($\approx 4\pi$ sr) so that optical emission-line and ionizing photons

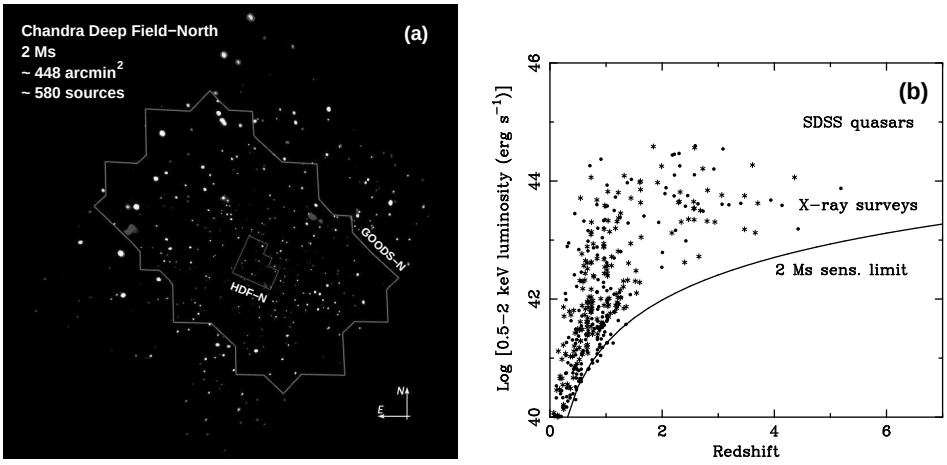

Figure 5. (a) Adaptively smoothed image of the 2 Ms CDF-N. Nearly 600 sources are detected in the $\approx$ 448 arcmin^2 field ($\approx$ 1/80000 the solid angle coverage of the SDSS). The regions covered by the HDF-N and GOODS-N surveys are denoted. Adapted from Alexander et al. (2003). (b) The $L_{\rm X}$–z plane with identified AGN in the CDF-N and CDF-S plotted. The solid curve shows the on-axis 0.5–2 keV luminosity detection limit for 2 Ms. Note that deep X-ray surveys can detect moderate-luminosity AGN out to $z > 6$, while the SDSS only detects the most luminous quasars.

cannot escape the nuclear region. XBONGs may be related to local elusive AGN such as NGC 4945 and NGC 6240 (e.g., Maiolino et al. 2003).

XBONGs are difficult to identify without X-ray data, and thus they may elude selection in the SDSS AGN survey. In fact, it was not possible to select the three XBONGs in the most intensively studied patch of sky, the Hubble Deep Field-North (HDF-N), prior to the *Chandra* observations (Brandt et al. 2001); these three XBONGs are among the brightest X-ray sources in the HDF-N.

Hundreds of archival hard X-ray observations combined with the SDSS should be powerful for finding local examples of XBONGs that can be studied in detail and hopefully placed within the unified model. Even if XBONGs are not selected in the SDSS AGN survey, $\gtrsim$200 with sensitive hard X-ray coverage may be "accidentally" targeted for spectra in the SDSS galaxy survey. Joint hard X-ray and SDSS investigations can thus clarify both the poorly understood size of the "true" XBONG population and the overall AGN selection effectiveness of the SDSS.

3.4. High-Redshift AGN Demography

Some of the most exciting SDSS advances have been on luminous high-redshift quasars (Fan et al., these proceedings), and substantial effort has been devoted to X-ray follow-up studies of these (e.g., Brandt et al. 2003; Bassett et al. and Vignali et al., these proceedings). A key finding from this work is that, even at the highest redshifts, the basic X-ray emission properties of quasars do not change strongly. This implies that X-ray AGN selection should remain effective

at high redshift, and it should be possible to combine the SDSS and X-ray surveys to explore high-redshift AGN demography. Sensitive X-ray surveys (e.g., Fig. 5a) can complement the SDSS since they can detect AGN that are $\gtrsim$10–30 times less luminous than the SDSS quasars (see Fig. 5b); these lower luminosity AGN are much more numerous and thus more representative than the rare SDSS quasars. Furthermore, X-ray surveys suffer from minimal absorption bias at high redshift where penetrating $\approx$ 2–40 keV rest-frame X-rays are accessed.

Follow-up studies of moderate-luminosity X-ray AGN at $z > 4$ are challenging, but some progress has been made via large-telescope spectroscopy and Lyman break selection (e.g., Barger et al. 2003; Cristiani et al. 2003; Koekemoer et al. 2003). There are unlikely to be more than ≈ 8 AGN at $z > 4$ detectable in a ≈ 1 Ms *Chandra* field, and the combined SDSS and X-ray results indicate that the AGN contribution to reionization at $z \approx 6$ is small. Additional deep ($\gtrsim$250 ks) *Chandra* observations are needed to provide more solid angle coverage at sensitive flux levels, so that the AGN luminosity-function shape can be determined at levels below those accessible to the SDSS; one such project, the Extended *Chandra* Deep Field-South, has recently been accepted for observation. Ultimately the SDSS, deep X-ray surveys, and wider X-ray surveys (e.g., ChaMP; see Silverman et al. 2002) should be able to define the $z > 4$ AGN luminosity function over a range of ≈ 1000 in luminosity.

4. Future Prospects

Future prospects for combined X-ray and SDSS studies appear wonderful! *Chandra*, *XMM-Newton*, and the SDSS all continue to generate torrents of superb data. *Chandra* and *XMM-Newton* should each deliver several thousand additional observations, and as the SDSS covers an increasingly large solid angle the synergy with archival X-ray data becomes increasingly potent. The selected topics in §2 and §3 represent only a sampling of the science that should be enabled; equally exciting research is expected on Narrow-Line Seyfert 1s, double-peaked line emitters, low-luminosity AGN, high-redshift quasars, type 2 quasars, and BAL quasars (just to name a few examples).

Future X-ray missions, some to be launched soon, will further increase combined X-ray and SDSS science opportunities. The SDSS should be of utility, for example, in follow-up investigations of many of the AGN detected in the $\approx$ 10–150 keV *Swift* Burst Alert Telescope sky survey. *Astro-E2* should allow high-quality iron Kα spectroscopy of selected X-ray bright SDSS AGN. In the more distant future, X-ray missions such as *Constellation-X*, *XEUS*, and *Generation-X* should enable efficient high-quality X-ray spectroscopy for most SDSS AGN.

Acknowledgments. We thank G. Risaliti and B.J. Wilkes for helpful discussions. Support from NASA LTSA grant NAG5-13035 (WNB, DPS), NSF CAREER award AST-9983783 (WNB), and NSF grant AST-9900703 (DPS) is gratefully acknowledged.

References

Alexander, D.M., et al. 2003, AJ, 126, 539

Anderson, S.F., et al. 2003, AJ, in press (astro-ph/0305093)

Barger, A.J., Cowie, L.L., Mushotzky, R.F., & Richards, E.A. 2001, AJ, 121, 662

Barger, A.J., Cowie, L.L., Capak, P., Alexander, D.M., Bauer, F.E., Brandt, W.N., Garmire, G.P., & Hornschemeier, A.E. 2003, ApJ, 584, L61

Brandt, W.N., Laor, A., & Wills, B.J. 2000, ApJ, 528, 637 (BLW)

Brandt, W.N., et al. 2001, AJ, 122, 1

Brandt, W.N., et al. 2003, Adv. Space Res., in press (astro-ph/0212082)

Brinkmann, W., Wang, T., Matsuoka, M., & Yuan, W. 1999, A&A, 345, 43

Comastri, A., et al. 2002a, ApJ, 571, 771

Comastri, A., et al. 2002b, in New Visions of the X-ray Universe in the *XMM-Newton* and *Chandra* Era (Noordwijk: ESA Press), in press (astro-ph/0203019)

Cristiani, S., et al., ApJ, in press (astro-ph/0309049)

Gallagher, S.C., Brandt, W.N., Laor, A., Elvis, M., Mathur, S., Wills, B.J., & Iyomoto, N. 2001, ApJ, 546, 795

Hagen, H.-J., Groote, D., Engels, D., & Reimers, D. 1995, A&AS, 111, 195

Hornschemeier, A.E., et al. 2001, ApJ, 554, 742

Kaspi, S., et al. 2002, ApJ, 574, 643

Koekemoer, A.M., et al., ApJ, in press (astro-ph/0306407)

Laor, A., & Brandt, W.N. 2002, ApJ, 569, 641

Maiolino, R., et al. 2003, MNRAS, 344, L59

Moran, E.C., Filippenko, A.V., & Chornock, R. 2002, ApJ, 579, L71

Richards, G.T., et al. 2003, AJ, 126, 1131

Risaliti, G., Elvis, M., Gilli, R., & Salvati, M. 2003, ApJ, 587, L9

Schmidt, M., & Green, R.F. 1983, ApJ, 269, 352

Schneider, D.P., et al. 2002, AJ, 123, 567

Severgnini, P., et al. 2003, A&A, 406, 483

Silverman, J.D., et al. 2002, ApJ, 569, L1

Vignali, C., Brandt, W.N., & Schneider, D.P. 2003a, AJ, 125, 433

Vignali, C., et al. 2003b, AJ, 125, 2876

Vignali, C., et al. 2003c, AJ, 125, 418

Wilkes, B.J., Tananbaum, H., Worrall, D.M., Avni, Y., Oey, M.S., & Flanagan, J. 1994, ApJS, 92, 53

Wilkes, B.J., Schmidt, G.D., Cutri, R.M., Ghosh, H., Hines, D.C., Nelson, B., & Smith, P.S. 2002, ApJ, 564, L65

Yuan, W., Brinkmann, W., Siebert, J., & Voges, W. 1998, A&A, 330, 108